Respiratory Physiology & Neurobiology 268 (2019) 103247

Contents lists available at ScienceDirect

Respiratory Physiology & Neurobiology

journal homepage: www.elsevier.com/locate/resphysiol

Distinct neural-mechanical efficiency of costal and crural diaphragm during hypercapnia

Giovanni Tagliabue, Michael Ji, Jenny V. Suneby Jagers, Dan J. Zuege, John B. Kortbeek, Paul A. Easton*

Department of Critical Care Medicine, Cumming School of Medicine, Calgary, University of Calgary, 2500 University Drive NW, Calgary, Alberta, T2N 4N1, Canada

ARTICLE INFO

Keywords:
Respiratory muscles
Diaphragm
Respiratory mechanics
EMG
Neural mechanical efficiency

ABSTRACT

Classic physiology suggests that the two distinct diaphragm segments, costal and crural, are functionally different. It is not known if the two diaphragm muscles share a common neural mechanical activation.

We hypothesized that costal and crural diaphragm are recruited differently during hypercapnic stimulated ventilation, and the EMG recordings of the esophageal crural diaphragm segment does not translate to the same level of mechanical shortening for costal and crural segments

In 30 spontaneously breathing canines, without confounding anesthetic, we measured directly electrical activity and corresponding mechanical shortening of both the costal and crural diaphragm, at room air and during increasing hypercapnia.

During hypercapnic ventilation, the costal diaphragm showed a predominant recruitment over the crural diaphragm. The distinct mechanical contribution of the costal segment was not due to a different level of neural activation between the two muscles as measured by segmental EMG activity. Thus, the two diaphragm segments exhibited a significantly different neural-mechanical relationship.

1. Introduction

There is increasing clinical interest in recording respiratory muscle EMG, especially diaphragm, as an indicator of ventilatory drive which can be utilized to guide mechanical ventilatory support and respiratory muscle monitoring (Vagheggini et al., 2013; Doorduin et al., 2013). The success of this important innovation depends on two crucial underlying assumptions. First, any measurement of EMG must truly reflect the respiratory neural activity driving the major respiratory muscles. And, secondly, the recorded EMG must faithfully reflect not just resting ventilatory drive, but the dynamic increasing neural activity in respiratory failure.

These essential preconditions present challenges for current and proposed clinical surface EMG recordings. For example, current clinical technique utilizes surface esophageal EMG which inevitably reflects predominantly crural diaphragm activity (Sinderby et al., 1999). Alternatively, recent attempts to utilize chest wall surface EMG may deduce lateral costal EMG activity but faces unavoidable interference from the intervening chest wall (Sinderby et al., 1996). Although both of these different diaphragm EMG methods should be possible, how can we be certain of clinical success and real validity of the methods to reflect the respiratory drive to the diaphragm? Is there a “reference standard” that can define and quantify by direct measurement, the neural activity and resultant mechanical action of the diaphragm, both at rest and during respiratory failure?

It is the aim of this project to define exactly the inherent EMG activity and mechanical action of both costal and crural diaphragm segments, from direct recordings within the respective muscles, in a normal intact mammal, during wakefulness without confounding anesthetic (Fitting et al., 1987), both at rest and during progressive hypercapnia as would be encountered during respiratory failure. If this activity of the diaphragm can be defined, then the validity of any proposed indirect measurement of diaphragm function, including surface EMG, can be compared and validated.

In our previous studies, using a canine model, we found some differential activity between the two portions of the diaphragm during hypercapnia (Easton et al., 1995). However, these previous studies were limited by the small number of subjects and the use of tracheostomy. The aim of this more complete study is to rigorously examine, in a large unanesthetized animal sample with intact airway, the specific neural mechanical contribution of the costal and crural portion of the diaphragm during hypercapnic ventilation. The use of the

* Corresponding author at: Department of Critical Care Medicine - University of Calgary, 2500 University Drive NW, Calgary, Alberta, T2N 1N4, Canada.
E-mail address: peaston@ucalgary.ca (P.A. Easton).

https://doi.org/10.1016/j.resp.2019.06.004
Received 4 December 2018; Received in revised form 30 May 2019; Accepted 23 June 2019
Available online 24 June 2019
1569-9048/

intramuscular electrode, which is the gold standard for EMG measurement, and sonomicrometry transducer (to measure directly length and shortening) in the costal and crural segment allow measurement of the electrical mechanical relationship of each segment of the diaphragm (Newman et al., 1984). This technique is invasive and, therefore, unsuitable for human studies. We used this model to address the following questions:

1) is the electrical signal of costal and crural portions of the diaphragm identical?

2) is the neural-mechanical efficiency of costal and crural diaphragm portions the same?

2. Methods

2.1. Ethical approval

All experimental procedures and protocols were performed in accordance with the *Canadian Council on Animal Care* (CCAC) Guideline. Experimental procedures were approved by the University of Calgary Animal Care Committee. All measurements of ventilation and respiratory muscle function were performed with the animals awake, relaxed and familiar with the location, routine and personnel of the recordings. No animal was euthanized at the end of the experiment.

2.2. Surgical preparation

Thirty mongrel canines (mean weight 23 kg) had sonomicrometry transducers and EMG wires implanted during laparotomy into costal and crural diaphragm segments, and were studied after full recovery of diaphragm segmental shortening (Easton et al., 1989). This implantation technique has been described elsewhere (Easton et al., 1989; Katagiri et al., 1994). Briefly, implantation of transducers and electrodes was performed under general anesthesia. The left hemidiaphragm was exposed through a midline abdominal incision, and ultrasonic transducers were implanted between muscle fibers on a flat portion of each of the costal and crural segments of the left hemidiaphragm. Costal transducers were placed in the lateral portion of the segment, approximately midway between central tendon and chest wall. Crural transducers were placed in the posterior, perivertebral region of the segment. Immediately adjacent to each transducer, a fine wire stainless steel bipolar EMG electrode was attached. All implants were secured by fine, synthetic, non-fibrotic sutures (Prolene, Ethicon, Somerville, NJ) and were externalized by a subcutaneous skin tunnel. Animals were allowed to fully recover prior to the measurements of resting and hypercapnic stimulated breathing.

Data reported here is retained in a physiologic digital database created in 2009.

2.3. Measurement techniques

Measurements of resting and CO_2-stimulated ventilation were made 22 ± 12 days post implantation, as detailed elsewhere (Easton et al., 1995). Measurements were performed with the animals awake, relaxed, and breathing quietly lying in the right lateral decubitus position, through a snout mask, attached through a 2-way non-rebreathing valve to a low-resistance closed breathing circuit connected to a pneumotachograph to provide inspiratory airflow (Fig. 1). On the expiratory limb, CO_2 was sampled continuously. Ventilatory and diaphragmatic responses to progressive hypercapnia were elicited by a modified Read technique, rebreathing 6% CO_2 - 94% O_2 from a 4-5-liter bag (Read, 1967; Rebuck and Read, 1971). Dynamic measurement of the distance between sonomicrometry transducers was provided by a sonomicrometer (Easton et al., 1989). EMG signals from the wire electrodes were amplified, band-pass filtered (16 Hz-l.6 KHz), rectified and "integrated" (time constant 100 ms) to provide moving average EMG of the diaphragm (Easton et al., 1995).

Measurements were made for airflow and breathing pattern in n = 30 animals. Costal and crural EMG signals were in n = 27 and n = 28 animals, respectively. Durability of sonomicrometry implants was not universal; costal and crural sonomicrometer signals were in n = 26 and n = 24 animals, respectively. Finally, n = 19 subjects had both costal and crural with matching paired EMG and sonomicrometer signals.

2.4. Analysis of ventilation

Using computer software for data acquisition (DataSponge), signals were monitored in real time on display and simultaneously collected, then analyzed using software written by one author (PAE), adapted to this project by a second author (MJ).

The flow signal was evaluated for respiratory timing and digitally integrated; breathing pattern was calculated breath-by-breath. Using the continuous sonomicrometer signal, the computer algorithm identified for each individual breath, the exact muscle length of costal and crural segments, which corresponded to the moment of onset of inspiratory flow. (L_{BL}) in millimeters and shortening per breath expressed as percent change from resting length (%L_{BL}). EMG activity was quantified per breath as maximum difference in volts between end-expiratory baseline and peak height of the moving average signal (EMG_{DIFF}). All muscle length, shortening and EMG activity were calculated at resting ventilation and four levels of CO_2.

2.5. Statistical analysis

After computer analysis, values were exported to spreadsheet and to SAS for statistical analysis (SAS/STAT, 2010). Mean values of breathing pattern, segmental length, shortening, and EMG activity were tested across resting and four levels of CO_2, by two-way ANOVA with repeated measures on one factor (Keppel, 1982). Multiple comparison testing of mean values was performed using Tukey's test (Steel and Torrie, 1980). Mean costal and crural shortening at each level of CO_2 were compared by paired t-test. Ventilatory, segmental shortening and EMG responses to hypercapnia were calculated by Pearson's correlation analysis. The slopes of costal and crural shortening and EMG were compared by paired t-test.

3. Results

3.1. Ventilatory response to hypercapnia

For the group, hypercapnic stimulus commenced at room air: $PETCO_2$ 38.08 ± 2.07 and terminated at highest CO_2 level: $PETCO_2$ 62.93 ± 1.93 mmHg. Variables describing the ventilatory pattern and peak tidal whole breath performance of the mechanical and electrical function of the diaphragm are summarized at these two extremes as well as three intermediate $PETCO_2$ values: 46.62 ± 1.02, 53.26 ± 1.64, 57.60 ± 2.04 mmHg (Table 1). For the group, awake and breathing spontaneously in the right lateral decubitus position after full recovery from implantation, minute ventilation (V_I) increased from baseline 8.84 ± 2.50 to 22.93 ± 6.15 L/min ($P < 0.001$), while tidal volume (V_T) increased from 0.36 ± 0.08 to 0.82 ± 0.20 L ($P < 0.001$). Across the range of CO_2 stimulation, the mean ΔV_I / $\Delta PETCO_2$ was 0.56 ± 0.24 L/min/mmHg.

3.2. Real-time display of costal and crural action

Throughout these recordings of resting and stimulated breathing, action of each diaphragm segment, including EMG activity and muscle shortening, was continuously monitored on-screen in real-time. As illustrated in Fig. 2, there was an obvious difference between the costal and crural diaphragm. Specifically, both segments showed equivalent peak EMG activation at rest and hypercapnic stimulation. By contrast,

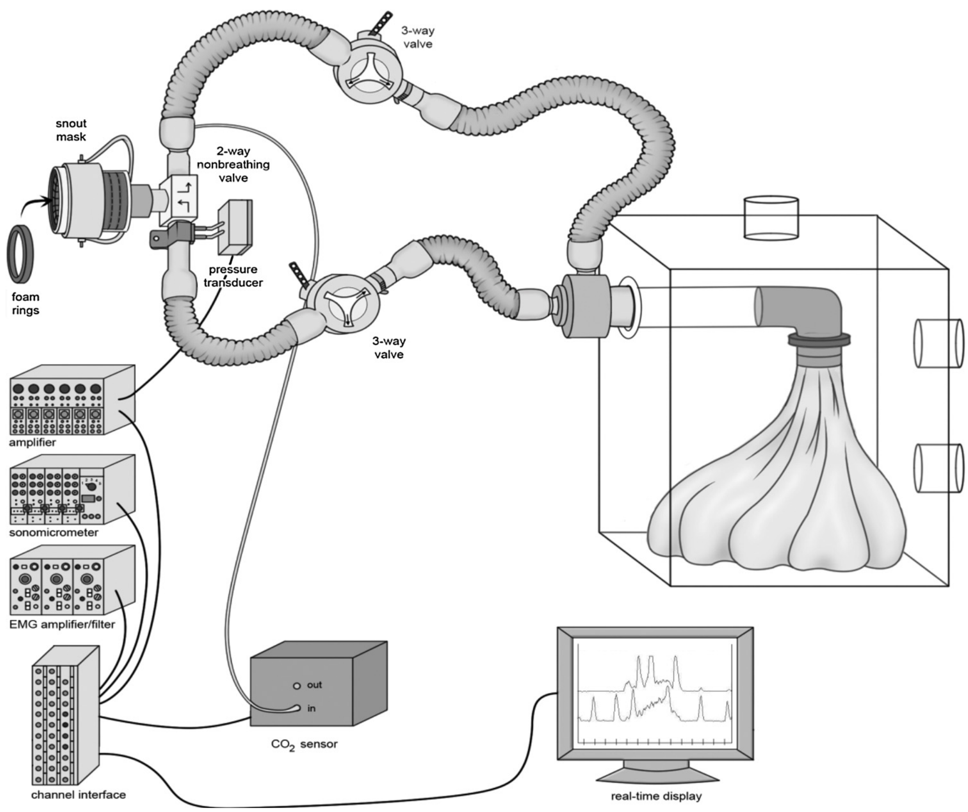

Fig. 1. CO_2 Rebreathing Circuit Model.
Circuit for measurement of ventilatory response to hypercapnia. Small 5 L meteorological balloon filled with 6% CO2 in 94% O_2 connected to a closed breathing circuit. Subject interface via snout mask filled with foam rings. Inspiratory and expiratory limbs, open to room air or rebreathing balloon by 3-way valves, connected to a plexiglass CO_2 rebreathing box. Pressure transducer for Fleisch #2 pneumotachograph connected to the inspiratory limb by a 2-way non-rebreathing valve. Exhaled CO_2 was continuously measured in the expiratory limb. Recorded signals were amplified, filtered and interfaced to a computerized analog-digital system for real-time display and continuous storage.

there was a clear difference in the magnitude of muscle shortening, between the two segments, with obviously greater shortening per EMG arising from the costal segment compared to the crural. Thus, neural recruitment as indexed by EMG was similar for the costal and crural diaphragm, but this equivalent neural activation did not translate into identical mechanical output. This compelling visual observation of divergent costal and crural diaphragm action was confirmed by the analysis described in following sections.

3.3. *Costal and crural have different neural-mechanical action*

The electromechanical responsiveness to CO_2 stimulation of the costal and crural diaphragm was overall linear (r = 0.99, $P < 0.0002$ for costal; r= 0.97, $P < 0.0052$ for crural), with the resultant slope of the shortening-EMG relationship - from room air and across the four levels of $PETCO_2$ - being slope ± SE 2.69 ± 0.12 vs 1.48 ± 0.20 % L_{BL}/V, respectively (Fig. 3). This electromechanical relationship during CO_2 stimulation was consistent within each animal and significantly different between the costal and crural segments ($P < 0.036$). For the group, there is also a notable divergence in the mechanical effectiveness

Table 1
Breathing pattern and diaphragm action at rest and during hypercapnia.

		Rest		Hypercapnia		
$P_{ET}CO_2$, mmHg		38.1 ± 2.1	46.6 ± 1.0	53.3 ± 1.6	57.6 ± 2.0	63 ± 2
V_I, L/min		8.84 ± 2.50	10.20 ± 2.58	14.13 ± 4.33	18.31 ± 5.81	22.93 ± 6.15
f, breaths/min		25.05 ± 7.08	23.48 ± 6.61	24.32 ± 7.87	26.22 ± 8.85	29.00 ± 8.33
V_T, L		0.36 ± 0.08	0.45 ± 0.10	0.60 ± 0.17	0.73 ± 0.20	0.82 ± 0.20
T_I, s		1.10 ± 0.29	1.17 ± 0.24	1.21 ± 0.27	1.20 ± 0.29	1.13 ± 0.25
T_I/T_{TOT}		0.43 ± 0.07	0.43 ± 0.15	0.46 ± 0.15	0.49 ± 0.16	0.51 ± 0.06
V_T/T_I, L/s		0.34 ± 0.08	0.38 ± 0.07	0.50 ± 0.11	0.61 ± 0.13	0.73 ± 0.16
Length L_{BL}, mm						
	COS	9.28 ± 2.15	9.29 ± 2.17	9.29 ± 2.17	9.30 ± 2.18	9.34 ± 2.36
	CRU	9.14 ± 2.39	9.13 ± 2.38	9.12 ± 2.37	9.12 ± 2.37	8.90 ± 2.39
Shortening, $\%L_{BL}$						
	COS	2.64 ± 1.28	3.44 ± 1.45	4.90 ± 1.90	5.94 ± 1.81	7.60 ± 1.86
	CRU	3.38 ± 1.68	3.87 ± 1.81	4.82 ± 1.94	5.43 ± 1.94	6.18 ± 2.49
EMG_{DIFF}, V						
	COS	4.46 ± 1.65	5.05 ± 1.70	5.59 ± 1.77	6.10 ± 1.88	6.40 ± 1.60
	CRU	5.09 ± 1.28	5.70 ± 1.53	6.56 ± 1.66	7.11 ± 1.77	7.54 ± 1.90

Values are means ± SD. $PETCO_2$, partial pressure of end-tidal CO_2; V_E, minute ventilation; f, respiratory frequency; V_T, tidal volume; T_I, inspiratory time; $T_I/_{TOT}$, inspiratory fraction of respiration; V_T/T_I mean inspiratory flow; L_{BL}, baseline resting muscle length at end-expiration; Shortening (%LBL), segmental shortening per breath expressed as percentage change from baseline resting muscle length at end-expiration; EMG_{DIFF}, segmental EMG per breath quantified as the maximum difference between baseline and peak height of the integrated moving average EMG signal in volts, V; COS, costal segment; CRU, crural segment. (n = 30, breathing pattern; n = 26, COS shortening; n = 24, CRU shortening; n = 27, COS EMG_{DIFF}; n = 28, CRU EMG_{DIFF}).

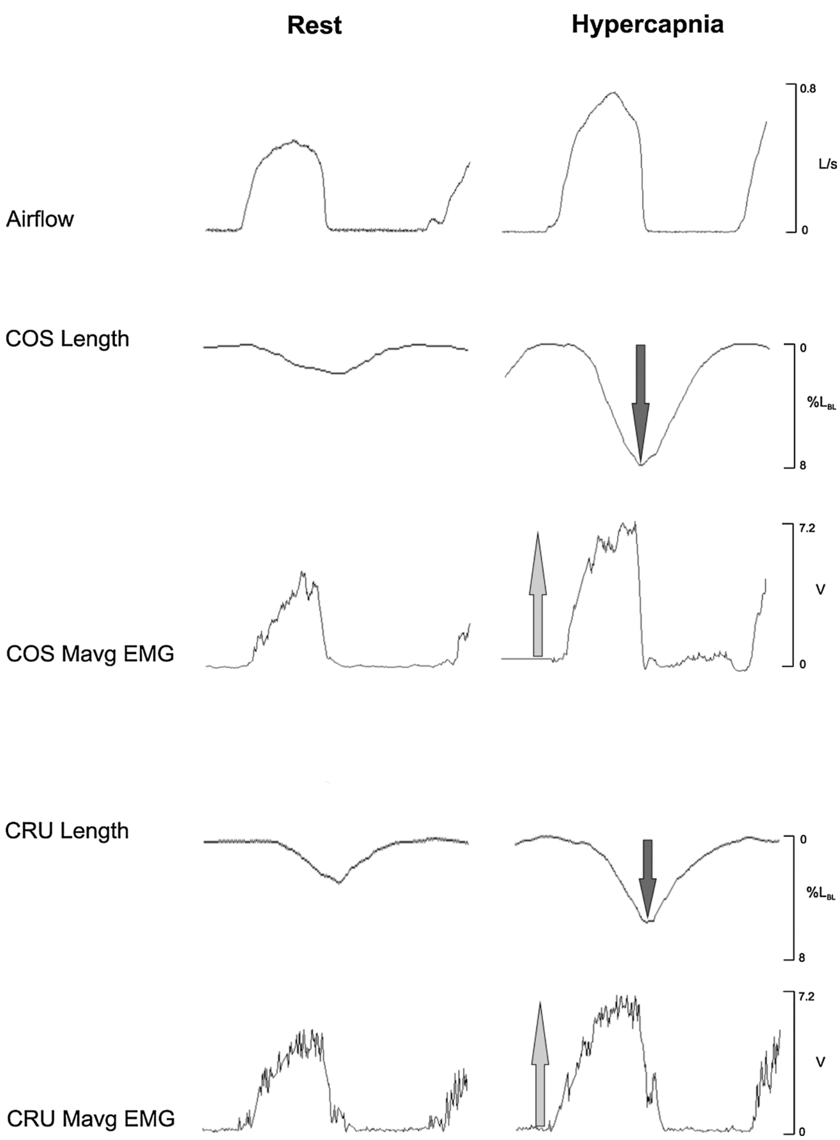

Fig. 2. Real-Time Display Shows Different Costal and Crural Action During Hypercapnia.

A typical recording of airflow and costal (COS) and crural (CRU) diaphragm, showing EMG activity and muscle shortening, during baseline room air rest (mean ˜38 mmHg) and hypercapnia (mean 63 mmHg). From *top* to *bottom*: airflow, shortening (%L_{BL}) and moving average EMG (Mavg EMG) of costal diaphragm, and shortening and moving average EMG of crural diaphragm. Grey arrows note an equivalent increase in EMG activity for both segments of the diaphragm from rest to hypercapnia; black arrows highlight the greater costal diaphragm shortening compared to crural.

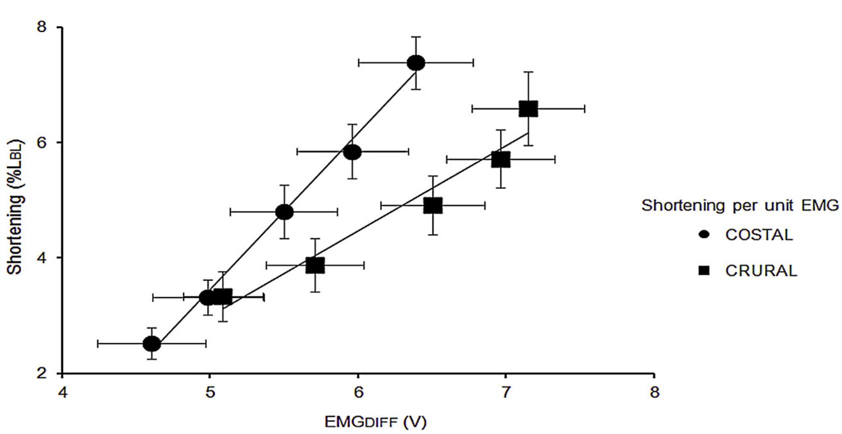

Fig. 3. Distinct Neural-Mechanical Action Between Costal and Crural Diaphragm.

The differing neuromechanical relation for costal and crural diaphragm. Mechanical shortening and EMG activity expressed per each diaphragm segment. Each point represents the neural-mechanical efficiency value of costal (circle) and crural (square) at room air (mean $PETCO_2$ ˜38 mmHg) and four levels of CO_2 stimulation (mean $PETCO_2$ ˜46, ˜53, ˜57, and 63 mmHg, respectively). The neural-mechanical relationship was linear (costal: r = 0.99, $P < 0.0002$ crural: r = 0.97, $P < 0.0052$) and significantly different between the two diaphragm segments (costal vs crural, slope: 2.69, standard error (SE) 0.12 vs 1.48 standard error (SE) 0.20%L_{BL}/V, $P < 0.0036$). EMG expressed as the maximum difference in volts between baseline and peak height of the moving average EMG signal (EMG_{DIFF}). Shortening expressed as percentage change from baseline resting length at end-expiration (%L_{BL}). Symbols show group mean values with standard error bars representing the standard error of the mean (SEM). Numerical labels express the magnitude of shortening and EMG_{DIFF} in absolute values (n = 19).

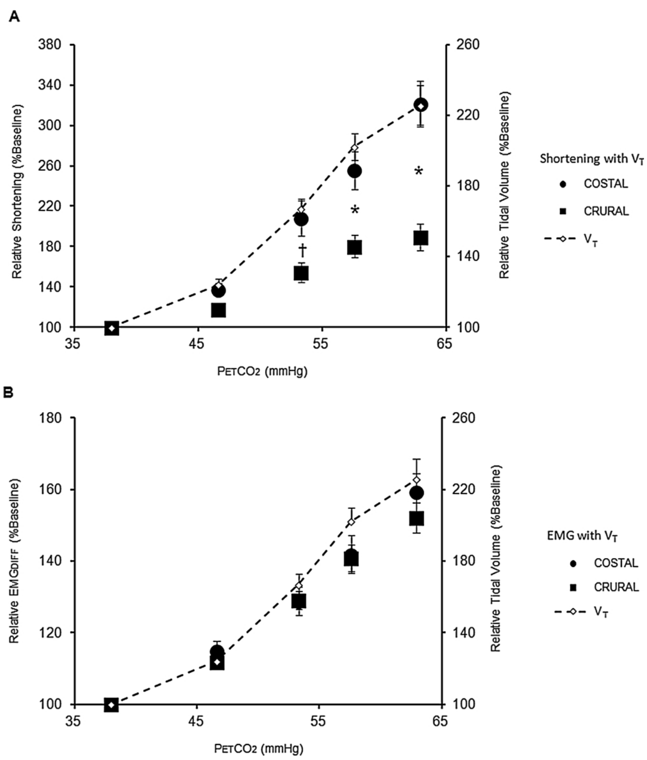

Fig. 4. Different Relative Shortening Between Costal and Crural Segments for the Same EMG.
Relative Values of Shortening and EMG of Costal and Crural Diaphragm during Rest and Hypercapnia. At room air and four level of CO_2 stimulation (values as in Fig. 3), costal (circle) and crural (square) values are expressed relative to the baseline value. A: segmental shortening of costal and crural expressed as percentage change of baseline shortening at room air (Relative Shortening). B: segmental EMG expressed as percentage change of baseline EMG_{DIFF} at room air (Relative EMG_{DIFF}). Dashed line: normalized tidal volume, V_T (percentage of baseline V_T at room air). Symbols are mean group values with standard error bars (SEM). Numerical labels express the magnitude of shortening and EMG_{DIFF} in relative values (A, n = 26, and n = 24; B, n = 27, and n = 28 for costal and crural, respectively). $PETCO_2$, end-tidal PCO_2. * p < 0.01 and † p < 0.05 between costal and crural segmental shortening/EMG for each $PETCO_2$ level, as noted by symbols.

of the two segments, as the costal portion appears to become progressively more "efficient" than the crural with greater EMG activation.

To ensure a robust matched comparison, this analysis only included animals that had paired EMG and muscle length signals from both diaphragm segments, i.e. costal EMG and shortening and crural EMG and shortening (n = 19). Subjects without a complete set including all four valid signals were excluded from this analysis. Since the shortening to EMG relationship represents the neuromuscular coupling of each diaphragm segment, this result reflects a fundamentally different neural-mechanical action of the two portions of the diaphragm during progressive hypercapnia.

3.4. Costal diaphragm contracts more than crural

For the whole group of subjects, costal and crural segmental shortening in absolute values ($\%L_{BL}$) increased significantly across all the levels of hypercapnia (costal: $P < 0.01$; crural: $P < 0.05$; Table 1). Accordingly, mean costal shortening increased from mean ± SD 2.64 ± 1.28 to 7.60 ± 1.86$\%L_{BL}$, while crural shortening increased from mean ± SD 3.38 ± 1.68 to 6.18 ± 2.49$\%L_{BL}$ (see Table 1). When comparing the relative change in the two muscles of the diaphragm as a percentage of resting baseline, costal showed significantly greater shortening than crural with progressive hypercapnic stimulation (costal vs crural at mean $PETCO_2$: ˜53 mmHg, $P < 0.05$; ˜57 mmHg, $P < 0.01$; and ˜62 mmHg, $P < 0.01$) (Fig. 4A).

3.5. EMG activity of costal and crural are equivalent

The group mean peak tidal moving average EMG measured from the costal and crural diaphragm increased significantly for both segments across the range of hypercapnia (costal and crural: $P < 0.01$; Table 1). At three intermediate values of $PETCO_2$ (mean ± SD 46.62 ± 1.02, 53.26 ± 1.64 and 57.60 ± 2.04 mmHg), and at the highest level of $PETCO_2$ (mean ± SD 62.93 ± 1.93 mmHg), the peak EMG of costal and crural increased consistently within each animal. In arbitrary voltage units, mean costal EMG increased from mean ± SD 4.46 ± 1.65 at rest to 6.40 ± 1.60 V at highest $PETCO_2$ level, while crural EMG increased from mean ± SD 5.09 ± 1.28 to 7.54 ± 1.90 V, respectively (Table 1). As a percentage from baseline resting activity, the relative difference in EMG is small and non-significant for the two portions of the diaphragm at each level of hypercapnic stimulation (Fig. 4B).

3.6. End-expiratory length of costal and crural does not change

To determine if the difference in muscle shortening between the two diaphragmatic segments was due to a more favorable force-length relation for the costal, we precisely measured the end-expiratory baseline length (L_{BL}) from which the costal and crural began to shorten with inspiration. For the entire group, mean L_{BL} ± SD was 9.28 ± 2.15 and 9.14 ± 2.39 mm at room air CO_2 of ˜38 mmHg for costal and crural segments, respectively. Across the whole range of CO_2 stimulation, the end-expiratory (or pre-inspiratory) baseline muscle length, L_{BL}, did not change significantly for either costal or crural segments. At the highest $PETCO_2$ of ˜62 mmHg, the L_{BL} was mean ± SD 9.34 ± 2.36 mm and 8.90 ± 2.39 mm for costal and crural segments, respectively. Even at the highest $P_{ET}CO_2$ level, the change in muscle length was extremely minimal compared to resting baseline.

4. Discussion

4.1. Data summary

In the current study, we focused our analysis on the electrical mechanical response to hypercapnia of a normal intact costal and crural diaphragm muscle, without confounding anesthetic. The main result of this study is during hypercapnic ventilation,costal shortening is significantly greater than crural shortening for the same level of neural activation directed towards the two diaphragm muscle segments.

4.2. Diaphragm segment differences

In animal and human, the costal and crural diaphragm present several points of differentiation (De Troyer et al., 1981). They originate from two separate embryological sites (Pickering and Jones, 2002), have a different distribution in fiber types (Reid et al., 1987; Sanchez et al., 1985) and have distinct innervations (Duron et al., 1979; Hammond et al., 1989; An et al., 2012). Functionally, costal and crural diaphragm can act as separate muscles. For instance, under specific physiologic conditions, the actions of the two segments can be opposite, notably during emesis (Abe et al., 1994) and panting (Easton et al., 1994). Moreover, in clinical situations, the generation of the neural drive is directly determined by the type (elastic and/or resistive) and degree of load on the respiratory system (Bradley, 1972; Lourenco et al., 1966; Gorman et al., 2005), and the pattern of distribution of the neural output among the respiratory muscles vary depending on the specific circumstances associated with the respiratory disease (Jolley et al., 2009; Liu et al., 2012). Within this context, it is plausible to hypothesize a distinct neural mechanical pattern even between the two portion of the diaphragm, costal and crural. If this would be the case, the clinical practice to use the EMG signal of a single respiratory muscle, the crural diaphragm segment, to infer neural drive and work of breathing of the entire respiratory system can be difficult to interpret.

4.3. Clinical diaphragm EMG monitoring

The clinical use of the electrical signal of the crural diaphragm (EAdi), by a dedicated nasogastric tube, has been introduced recently as a continuous monitoring tool, to assess the work load of the respiratory system. The use of the EAdi to infer the mechanical output relies on two main assumptions: 1) a linear relationship, for a wide range of submaximal diaphragm activation, between the EAdi and the diaphragm mechanical output, defined as neural mechanical or neural ventilatory efficiency (Beck et al., 1998; Bellani et al., 2013; Finucane et al., 2005; Beck et al., 2001); 2) an identical neural mechanical coupling between the two muscles composing the diaphragm, costal and crural, such that the EAdi alone is representative of both segments, thus the entire diaphragm (Sprung et al., 1989; Decramer et al., 1990). To the best of our knowledge, no previous study has specifically investigated these two assumptions - most of the supporting evidence is deduced from human clinical studies, using the EAdi as the sole electrical-myographic signal for representing the whole diaphragm.

On this background, the novel finding from this study is the predominant shortening/mechanical contribution of the costal over the crural diaphragm, despite the same level of neural recruitment, during physiologic hyperventilation. This implies distinct neural-mechanical action, differing between the two muscles of the diaphragm.

4.4. Directly measured diaphragm action

These measurements rely on the assumption that the fully recovered, awake, and spontaneously breathing canine with chronically implanted sonomicrometry transducers and EMG wires presents the normal function of the diaphragm segments at rest and when ventilation is stimulated by CO_2 (Easton et al., 1989). Segmental length change as recorded from the costal sonomicrometry transducers in these canines may represent shortening throughout the costal segment, as suggested in an early sonomicrometry study of the diaphragm in anesthetized dogs (Newman et al., 1984). However, recent evidence suggests that significant inter-regional and infra-regional differences in shortening may occur within the costal segment (Sprung et al., 1989). If such regional differences are operative in these animals, then these recordings of costal shortening are most representative of the central portion of the middle region of the costal segment, which, in agreement with Sprung et al. study, showed to have the larger shortening fraction of the entire costal diaphragm. (Sprung et al., 1989) It should be noted that, for the canines in this series, the positioning of the transducers along the costal segment, relative to the origin and central tendinous insertion, was always consistent. These recordings were uniformly done with the animals awake and positioned in right lateral decubitus. And, the change in respiratory muscle resting length between supine and lateral decubitus was found to be small. Further, the analysis of the end-expiratory length allows reasonable exclusion of any divergent force-length characteristic as the origin of the different degree of shortening between the costal and crural diaphragm.

The relative increase of costal and crural peak tidal EMG during hypercapnia was linear for both portions of the diaphragm and equivalent at rest and during different levels of hypercapnia. Since EMG was recorded simultaneously with the shortening activity from the same region of the costal and crural diaphragm from each animal, we can be confident that the significant difference in shortening between the two muscles is related to their inherent mechanical properties and structure rather than any divergent neuromotor output stimulation. To the best of our knowledge, this is the first study examining the electrical mechanical recruitment, during hypercapnia, of both portions of an intact in vivo diaphragm in any awake mammal.

4.5. Different segmental neural-mechanical action

If we use the relationship of shortening to EMG, i.e. the slope of shortening/EMGDIFF, to describe the neural mechanical efficiency, we might conclude that in a normal intact diaphragm, crural is inherently “less efficient” than costal diaphragm. However, this interpretation does not take in account unique neural-mechanical characteristic of each portion of the diaphragm and their potential interaction with each other and other respiratory muscles. (De Troyer et al., 1982).

Costal and crural diphragm segments are different in size and anatomical arrangement. Costal represents the largest portion of the surface area of the diaphragm relative to crural diaphragm and is attached anteriorly to the lower rib cage and posteriorly to the anterior portion of the central tendon. Crural is attached anteriorly to the posterior portion of the central tendon and posteriorly to the spine. Macklem et al. proposed a mechanical model where mechanically, costal and crural are arranged partially in series and, moving from functional residual capacity, partially in parallel. By that classic mechanics model, while the length of crural is determined exclusively by the displacement of central tendon costal diaphragm is determined both by the displacement of the central tendon and lower rib cage (Macklem et al., 1983). Therefore, the lower rib cage is arranged in series for the crural portion and partially in parallel for the costal portion, such that the shortening of one muscle cause the shortening of the other one (Macklem et al., 1983). Subsequently, Decramer et al. tested Macklem's model without conclusive results since only half of the subjects showed lower rib cage muscles and costal diaphragm interacting in series rather, as expected by Macklem et al. model, in parallel and no alternative hypothesis was postulated beyond the mechanical prospective (Decramer et al., 1984). It is of interest that is this current study, costal and crural baseline segmental length are unchanged through the entire hypercapnia stimulation. It is hard to hypothesize a scenario where lower rib cage interaction with costal diaphragm is altering length and shortening of costal diaphragm explaining a greater degree of shortening compared to crual diaphragm, yet baseline length of the two segments of the diaphragm throughout hypercapnia is unchanged. Also, the precise measurement of the end-expiratory length of the two portions of the diaphragm seems to be evidence against the possibility that crural shortening is less than costal because of a larger effect of abdominal muscles activation, through the central tendon, duirng hypercapnia (Abe et al., 1996).

An entirely different, contemporary, hypothesis, not based solely on classic mechanics, is that the functional difference shown in our study arises from distinct operational roles of the costal and crural diaphragm. Since Macklem and Decramer's work, several lines of evidence suggest costal and crural diaphragm have a distinct neural-mechanical profile. For instance, in dogs, during physiologic condition like panting or emesis the activation of costal and crural diaphragm is entirely different, even opposite, between the two segments of the diaphragm (Easton et al., 1994 and Abe et al., 1994). More recently, we have shown how neural activation of costal and crural diaphragm differ during acute and chronic hypoxia (Ikegami et al., 2019).

Although neurally distinct, costal and crural diaphragm share central tendon attachment. Thus the tension generated by the two segments of the diaphragm, at least in part, is distributed across the segments, reciprocally influencing their mechanics. For instance, during panting, the onset of crural activation is out of phase causing a significant decrease in tidal volume, which is, ultimately, generated only by costal diaphragm (Easton et al., 1994). The inspiratory shortening of costal would be proportional to the volume displaced by the diaphragm only if one attachment remain immobile relative to the other. This requirement is not met for the rib cage, as the lower costal margins move upward and outward; on the other side, the central tendon is pulled by the crural portion of the diaphragm. In these circumstances, the role of the crural would be critical by adjusting the central tendon to optimize the shortening of the costal diaphragm.

Finally, in this study we have limited our analysis of EMG and shortening to the whole tidal breath. However, we previously observed that during hypercapnia in early inspiration crural shortening consistently precedes costal shortening (Easton et al., 1993). Further dedicated studies are required in order to elucidate the intra-breath time domain differences of the costal and crural diaphragm.

4.6. Conclusion and clinical implications

Our findings suggest that, the use of the EMG electrical signal of one portion of the diaphragm to infer the mechanical action of the entire respiratory system can be difficult to interpret, and may be misleading. In clinical situations, the variation in EAdi arising predominantly from the crural may not represent the physical recruitment of the costal diaphragm. And thus, EAdi may not faithfully reflect the diaphragm generation of tidal volume, since costal diaphragm shows a greater recruitment compared to crural. Since the mechanical action of the two segments are distinct, it is reasonable to expect that in condition of altered respiratory work load, the neural activation between the two muscles may differ as well. The distinct neural mechanical profile of the costal and crural diaphragm may suggest that the two portions of the diaphragm have a distinct, albeit interacting, operational role in generating tidal volume.

Authors contributions

Conception or design of the work: P.A.E. Acquisition, analysis, or interpretation of the data for the work: G.T., M.J., J.V.S.J., D.J.Z., J.B.K., P.A.E. Drafting the work or revising it critically for important intellectual content: G.T.

All authors approved the final version of the manuscript and agree to be accountable for all aspects of the work in ensuring that quesions related to the accuracy or integrity of any part of the work are appropriately investigated. All persons designated as authors qualify for autorship, and all those who qualify for authorship are listed.

References

Abe, T., Kieser, T.M., Tomita, T., Easton, P.A., 1994. Respiratory muscle function during emesis in awake canines. J. Appl. Physiol. 76, 2552–2560. https://doi.org/10.1152/jappl.1994.76.6.2552.

Abe, T., Kusuhara, N., Yoshimura, N., Tomita, T., Easton, P.A., 1996. Differential respiratory activity of four abdominal muscles in humans. J. Appl. Physiol. 80, 1379–1389. https://doi.org/10.1152/jappl.1996.80.4.1379.

An, X., Yue, B., Lee, J.H., Lee, M.S., Lin, C., Han, S.H., 2012. Intramuscular distribution of the phrenic nerve in human diaphragm as shown by Sihler staining. Muscle Nerve 45, 522–526. https://doi.org/10.1002/mus.22141.

Beck, J., Sinderby, C., Lindstrom, L., Grassino, A., 1998. Effect of lung volume on diaphragm EMG signal strength during voluntary contractions. J. Appl. Physiol. 85, 1123–1134. https://doi.org/10.1152/Jappl.1998.85.3.1123.

Beck, J., Gottfried, S.B., Navalesi, P., Skrobik, Y., Comtois, N., Rossini, M., 2001. Electrical activity of the diaphragm during pressure support ventilation in acute respiratory failure. Am. J. Respir. Crit. Care Med. 164, 419–424. https://doi.org/10.1164/ajrccm.164.3.2009018.

Bellani, G., Mauri, T., Coppadoro, A., Grasselli, G., Patroniti, N., Spadaro, S., 2013. Estimation of patient's inspiratory effort from the electrical activity of the diaphragm. Crit. Care Med. 41, 1483–1491. https://doi.org/10.1097/CCM.0b013e31827.

Bradley, G.W., 1972. The response of the respiratory system to elastic loading in cats. Respir. Physiol. 16, 142–160. https://doi.org/10.1016/0034-5687(72)90047-3.

Decramer, M., De Troyer, A., Kelly, S., Macklem, P.T., 1984. Mechanical arrangement of costal and crural diaphragms in dogs. J. Appl. Physiol. 56, 1484–1490. https://doi.org/10.1152/japplphysiol.00242.2018.

De Troyer, A., Sampson, M., Sigrist, S., Macklem, P.T., 1981. The diaphragm: two muscles. Science 231, 237–238 https://doi.org/213, 237-238.

De Troyer, A., Sampson, M., Sigrist, S., Macklem, P.T., 1982. Action of costal and crural parts of the diaphragm on the rib cage in dog. J. Appl. Physiol. Respirat. Environ. Exercise Physiol. 53, 30–39. https://doi.org/10.1152/jappl.1982.53.1.30.

Doorduin, J., van Hees, H.W., van der Hoeven, J.G., Heunks, L.M., 2013. Monitoring of the respiratory muscles in the critically ill. Am. J. Respir. Crit. Care Med. 187, 20–27. https://doi.org/10.1164/rccm.201206-1117CP.

Duron, B., Marlot, D., Macron, J.M., 1979. Segmental motor innervation of the cat diaphragm. Neurosci. Lett. 15, 93–96. https://doi.org/10.1016/0304-3940(79)96095-6.

Easton, P.A., Fitting, J.W., Arnoux, R., Guerraty, A., Grassino, A.E., 1989. Recovery of diaphragm function after laparotomy and chronic sonomicrometer implantation. J. Appl. Physiol. 66, 13–21. https://doi.org/10.1152/jappl.1989.66.2.613.

Easton, P.A., Fitting, J.W., Arnoux, R., Guerratay, A., Grassino, A.E., 1993. Costal and crural diaphragm function during CO2 rebreathing in awake dogs. J. Appl. Physiol. 74, 1406–1418. https://doi.org/10.1152/jappl.1993.74.3.1406.

Easton, P.A., Abe, T., Young, R.N., Smith, J., Guerraty, A., Grassino, A., 1994. Costal and crural function during panting in awake canines. J. Appl. Physiol. 77, 1983–1990. https://doi.org/10.1152/jappl.1994.77.4.1983.

Easton, P.A., Abe, T., Smith, J., Fitting, J.W., Guerraty, A., Grassino, A.E., 1995. Activity of costal and crural diaphragm during progressive hypoxia or hypercapnia. J. Appl. Physiol. 78, 1985–1992. https://doi.org/10.1152/jappl.1995.78.5.1985.

Finucane, K.E., Panizza, J.A., Singh, B., 2005. Efficiency of the normal human diaphragm with hyperinflation. J. Appl. Physiol. 99, 1402–1411. https://doi.org/10.1152/japplphysiol.01165.2004.

Fitting, J.W., Easton, P.A., Arnoux, R., Guerraty, A., Grassino, A., 1987. Effect of anesthesia on canine diaphragm length. Anesthesiology 66, 531–536. https://doi.org/10.1097/00000542-198704000-00014.

Gorman, R.B., McKenzie, D.K., Butler, J.E., Tolman, J.F., Gandevia, S.C., 2005. Diaphragm length and neural drive after lung volume reduction surgery. Am. J. Respir. Crit. Care Med. 172, 1259–1266. https://doi.org/10.1378/chest.116.6.1593.

Hammond, C.G., Gordon, D.C., Fisher, J.T., Richmond, F.J., 1989. Motor unit territories supplied by primary branches of the phrenic nerve. J. Appl. Physiol. 66, 61–71. https://doi.org/10.1152/jappl.1989.66.1.61.

Ikegami, T., Ji, M., Fujmura, N., Suneby Jagers, J.V., Kieser, T.M., Easton, P.A., 2019. Costal and crural diaphragm function during sustained hypoxia in awake canines. J. Appl. Physiol. 7 (February). https://doi.org/10.1152/jappl.1984.56.6.1484. [Epub ahead of print].

Jolley, C.J., Luo, Y.M., Steier, J., Reilly, C., Seymour, J., Lunt, A., 2009. Neural respiratory drive in healthy subjects and in COPD. Eur. Respir. J. 33, 289–297. https://doi.org/10.1164/rccm.201402-0302LE.

Katagiri, M., Young, R.N., Platt, R.S., Kieser, T.M., Easton, P.A., 1994. Respiratory muscle compensation for unilateral or bilateral hemidiaphragm paralysis in awake canines. J. Appl. Physiol. 77, 1972–1982. https://doi.org/10.1152/jappl.1994.77.4.1972.

Keppel, G., 1982. The single factor within subject design. Design and Analysis: a Researcher's Handbook, 2nd ed. Prentice-Hall, Englewood Cliff., pp. 382–408.

Liu, L., Liu, H., Yang, Y., Huang, Y., Liu, S., Beck, J., 2012. Neuroventilatory efficiency and extubation readiness in critically ill patients. Crit Care 16, R143. https://doi.org/10.1186/cc11451.

Lourenco, R.V., Cherniack, N.S., Malm, J.R., Fishman, A.P., 1966. Nervous output from the respiratory center during obstructed breathing. J. Appl. Physiol. 21, 527–533. https://doi.org/10.1152/jappl.1966.21.2.527.

Macklem, P.T., Macklem, D.M., De Troyer, A., 1983. A model of inspiratory muscle mechanics. J. Appl. Physiol. Respir. Environ. Exerc. Physiol. 55, 547–557. https://doi.org/10.1152/jappl.1983.55.2.547.

Newman, S., Road, J., Bellemare, F., Clozel, J.P., Lavigne, C.M., Grassino, A., 1984. Respiratory muscle length measured by sonomicrometry. J. Appl. Physiol. 56, 753–764. https://doi.org/10.1152/jappl.1984.56.3.753.

Pickering, M., Jones, J.F., 2002. The diaphragm: two physiological muscles in one. J. Anat. 201, 305–312. https://doi.org/10.1046/j.1469-7580.2002.00095.x.

Read, D.J., 1967. A clinical method for assessing the ventilatory response to carbon dioxide. Australas. Ann. Med. 16, 20–32.

Rebuck, A.S., Read, J., 1971. Patterns of ventilatory response to carbon dioxide during recovery from severe asthma. Clin. Sci. 41, 13–21. https://doi.org/10.1042/cs0410013.

Reid, M.B., Ericson, G.C., Feldman, H.A., Johnson, R.L.Jr., 1987. Fiber types and fiber diameters in canine respiratory muscles. J. Appl. Physiol. 62, 1705–1712. https://doi.org/10.1152/jappl.1987.62.4.1705.

Sanchez, J., Medrano, G., Debesse, B., Riquet, M., Derenne, J.P., 1985. Muscle fiber types in costal and crural diaphragm in normal men and in patients with moderate chronic respiratory disease. Bull. Eur. Physiopathol. Respir. 21, 351–356.

Sinderby, C., Navalesi, P., Beck, J., Skrobik, Y., Comtois, N., Friberg, S., 1999. Neural control of mechanical ventilation in respiratory failure. Nature Med 5, 1433–1436. https://doi.org/10.1038/71012.

Sinderby, C., Friberg, S., Comtois, N., Grassino, A., 1996. Chest wall muscle cross talk in canine costal diaphragm electromyogram. J. Appl. Physiol. 81, 2312–2327. https://doi.org/10.1152/jappl.1996.81.5.2312.

Sprung, J., Dechamps, C., Hubmayr, R.D., Walters, B.J., Rodarte, J.R., 1989. In vivo regional diaphragm function in dogs. J. Appl. Physiol. 67, 655–662. https://doi.org/10.1152/jappl.1989.67.2.655.

Steel, R.G., Torrie, J.H., 1980. Principles and Procedures of Statistics: a Biometrical Approach, 2nd ed. McGrawHill, NewYork, pp. 172–194 102-104.

Vagheggini, G., Mazzoleni, S., Vlad, P.E., Navalesi, P., Ambrosini, N., 2013. Physiologic response to various levels of pressure support and NAVA in prolonged weaning. Respir. Med. 107, 1748–1754. https://doi.org/10.1016/j.rmed.2013.08.013.